Implications of vulnerability to hurricane damage for long-term survival of tropical tree species: a Bayesian hierarchical analysis

Kiona Ogle, María Uriarte, Jill Thompson, Jill Johnstone, Andy Jones, Yiching Lin, Eliot J.B. McIntire, and Jess K. Zimmerman

Tropical forests in the Caribbean are often subject to catastrophic disturbances by hurricanes. Despite the high frequency and intensity of hurricanes in this region, their effect on tropical forest dynamics remain poorly understood. In an effort to better understand the importance of hurricanes to a Puerto Rican tropical forest, we employ Bayesian statistical methods to identify factors that may determine the response of individual trees to hurricane damage. These factors include the effect of tree size and taxonomic identity on the vulnerability of trees to wind damage and the effect of wind damage, tree size, and crowding on individual survival following a hurricane event. In this analysis, we use data from the censuses of the 16-ha Luquillo Forest Dynamics Plot (LFDP) in Puerto Rico that include assessments of damage following Hurricane Hugo (Sept. 1989), status (alive or dead) 2–5 years after Hugo, size, neighborhood crowding, and spatial location for each tree. At the species level, the association between life-history traits and structural attributes generate a positive relationship between shade tolerance and resistance to hurricane damage. We focus our analyses on four relatively common tree species in the LFDP that represent a range of life-history strategies: shade intolerant, early successional species *Alchornea latifolia* and *Casearia arborea*, and shade tolerant species *Dacryodes excelsa* and *Manilkara bidentata*. At the stand level, spatial variation in storm severity is an important driver of individual tree damage, but its direct effects are difficult to separate from other landscape-level factors that interact with hurricane intensity to affect tree survival. In this study we build a hierarchical, spatially explicit Bayesian model that provides a straightforward method for evaluating species-specific susceptibility to hurricane damage and the implications for survival. We apply the method as a tool to quantify stand-level spatial variability in hurricane intensity, independent of species composition and stand age or size structure.

6.1 Introduction

Hurricanes represent the dominant natural perturbation in tropical forests of the Caribbean islands (e.g. Walker et al. 1991; Zimmerman et al. 1994; Walker et al. 1996). Disturbance theories have generally distinguished catastrophic, large-scale disturbances as a result of external forces (e.g. hurricanes) from small-scale disturbances within communities (e.g. tree falls) (e.g. Brokaw 1985; Pickett et al. 1989). It has become clear that this dichotomy is not a useful model for understanding the effects of hurricane disturbance in tropical forests because hurricanes vary greatly in their intensity and the severity of their impact over a range of spatial and temporal scales (Boose et al. 1994).

Storm meteorology, proximity to the storm's center, and topography are obvious factors that generate large-scale variation in damage that may range from limited localized canopy damage to widespread uprooting of trees. At smaller spatial scales, the distribution of hurricane-induced damage within a particular forest varies with species composition and forest structure (Boose et al. 1994). This small-scale heterogeneity is in part generated by species-specific variation in: (1) susceptibility to damage from winds of a given intensity, (2) the nature of the damage incurred as a function of wind speed, and (3) the ability and rate of recovery from hurricane damage at the level of both the individual plant (through repair of damage, resprouting, rapid leaf area production) and the population (through reproduction, seedling establishment, and juvenile response to improved resource availability such as enhanced light intensity) (e.g. Glitzenstein and Harcombe 1988; Peterson and Pickett 1991; You and Petty 1991; Boucher et al. 1994; Zimmerman et al. 1994; Peterson and Rebertus 1997; Cooper-Ellis et al. 1999). Species-specific traits in response to damage interact with landscape-level variation in severity of damage to create complex spatial patterns that affect both short- and long-term community dynamics of these tropical forests. To separate forest stand structure and species effects from the spatial distribution of storm characteristics, we need analytical approaches that are capable of combining spatially extensive and temporally intensive forest inventory data sets that span a range of temporal and spatial scales (Canham et al. 2001).

Predicting the long-term effects of hurricanes on forest dynamics is difficult. At the level of an individual tree, many factors interact to influence the likelihood that a particular tree will be affected by a hurricane, including: (1) species-specific structural and biomechanical traits (e.g. wood density, flexibility of the stem, root and crown architecture, King 1986; Zimmerman et al. 1994; Harrington and DeBell 1996; Peltola et al. 1999; Uriarte et al. 2004), (2) the size of the tree (e.g. Zimmerman et al. 1994; Stokes 1999), and (3) local storm intensity (wind speed and turbulence) (e.g. King 1986; Gardiner et al. 2000). In theory, an index of the average level of observed damage experienced by all trees in an area can be used as a surrogate for storm intensity, assuming

that the severity of damage (e.g. biomass loss) is proportional to storm force. This is a reasonable approach when the plots contain a well-mixed sample of species and tree sizes. In the field, however, some forest areas may appear to have been subjected to strong winds simply because they are dominated by species or size classes that are particularly vulnerable to wind damage (Canham et al. 2001). This complication hinders our ability to obtain good estimates of local storm intensity and, therefore, to predict species-specific variation in susceptibility to damage. Local storm intensity is particularly difficult to disentangle in tropical forests because of the large number of species that may coexist in a small area, each of which may respond differently to wind disturbance. Additionally, practically no two neighborhoods in a tropical forest have similar species compositions or abundances (Hubbell and Foster 1986).

Although global warming may increase the frequency and severity of hurricanes in the Caribbean in the long term (Henderson-Sellers et al. 1998), a greater and more immediate concern is a recent five-fold increase in hurricane activity during the past decade (Goldenberg et al. 2001). This increase appears to be part of a pattern of multidecadal oscillations in sea surface temperature over the Atlantic that is likely to continue for 10–30 years (Goldenberg et al. 2001). Forests of Puerto Rico may be particularly affected by an increase in the number of hurricane events because the island already experiences one of the highest hurricane frequencies in the Caribbean (Boose et al. 2004). In September 1989, Hurricane Hugo passed over the northeastern corner of Puerto Rico, striking forests on the island with maximum sustained winds of 166 km/h and gusts of 194 km/h (Scatena and Larsen 1991). Hurricanes of similar severity to Hugo affect Puerto Rico every 50–60 years on average (Scatena and Larsen 1991), but this frequency is likely to increase (Goldenberg et al. 2001), requiring a better understanding of the effects of hurricane disturbance on tropical forest structure and function, particularly in this region.

Improving our understanding of the impacts that hurricanes have on tree survival is critical to predicting the effects of hurricane damage on forest dynamics. This requires that we consider the primary factors that are likely to influence the
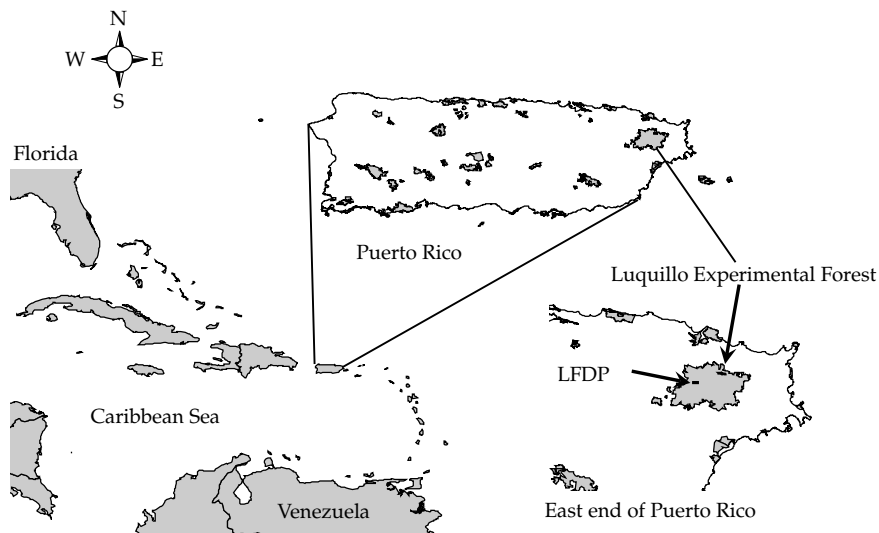
Figure 6.1. Location of the LFDP within Puerto Rico. The gray patches within Puerto Rico are forest reserves. The LFDP is indicated by the small black mark within the Luquillo Experimental Forest.

survival of individual trees in the presence and absence of hurricane damage, including tree size and the intensity of competition between trees for resources such as light and nutrients. In this paper we take advantage of data collected immediately following Hurricane Hugo and apply a Bayesian approach to simultaneously consider the chief factors likely to determine the probability that an individual tree will survive the post-hurricane recovery period. These are: (1) the effects of taxonomic identity and tree size on vulnerability to hurricane damage, (2) the influence of hurricane damage on subsequent tree survival, and (3) the effects of tree size and crowding (a surrogate for the level of competition) on survival, independent of hurricane damage. We also use the approach to infer the spatial pattern in storm intensity at the forest stand level, after accounting for variation in damage due to the distribution tree sizes and species composition (with respect to the four species included in this analysis) and stand density (in terms of basal area of all species in the LFDP).

6.2 Field Study

The LFDP, previously known as the Hurricane Recovery Plot (Zimmerman et al. 1994), is a 16-ha forest plot (SW corner 18°20′N, 65°49′W) located near El Verde Field Station in the Luquillo Mountains of northeastern Puerto Rico (Figure 6.1). The plot is 500 m N–S and 320 m E–W and is divided into 400 (20 m × 20 m) quadrats (Thompson et al. 2002). Vegetation and topography of the local area is typical of the tabonuco (*Dacryodes excelsa*) forest zone. The forest is classified as subtropical wet by the Holdridge life zone system (Ewel and Whitmore 1973) and tropical montane by Walsh's (1996) tropical climate system. Rainfall averages 3500 mm per year, and elevation ranges from 333 to 428 m a.s.l. All of the soils are formed from volcaniclastic rock (Soil Survey Staff 1995).

The LFDP is characterized by spatially segregated land-use histories. Much of the forest was altered by logging and agricultural activity until ca. 1934 when the US Forest Service (USFS) acquired the land (Thompson et al. 2002). The mapped stand spans areas that suffered differing degrees of disturbance resulting from clear-cutting and agriculture, but also includes a relatively undisturbed portion that was subjected to a small amount of selective logging in the 1940s (Thompson et al. 2002). Land-use history influences the spatial pattern of hurricane damage because the species that colonize logged or abandoned agricultural areas tend to be more vulnerable

to hurricanes than those growing in unaltered stands (Thompson et al. 2002; Boose et al. 2004).

The LFDP was established and surveyed after Hurricane Hugo, and Thompson et al. (2002) provide a detailed description of the sampling design and census methods. A survey of the impact of Hurricane Hugo in the LFDP was conducted between September 1990 and February 1991 by assessing all trees ≥10 cm in DBH (diameter at breast height, ca. 1.3 m from the ground) for the degree of damage suffered during Hurricane Hugo. Damage (D) was coded for this analysis as: undamaged or light damage ($D = 0$); partial damage, a combination of branch and crown breakage, but no damage to the main stem ($D = 1$); or heavily damaged such as a snapped stem or uprooting ($D = 2$). Damaged, leafless trees were identified to species based on bark characteristics and tree form. An extensive inventory of all stems ≥10 cm in DBH was conducted from June 1990 until February 1992, during which period trees were tagged, explicitly mapped within the plot, identified to species, and their DBH was measured. Species identities were determined by sight in the field or from voucher specimens following nomenclature of Liogier (1985, 1988, 1994, 1995, 1997). An inventory of small stems (1 cm ≤ DBH < 10 cm) was conducted between February 1992 and September 1993. These small trees, many of which were recruited after Hurricane Hugo and were not assessed for damage, were

tagged, identified, measured for DBH, and their location within the plot was assigned to a 5 m × 5 m subquadrat. These two inventories of all trees ≥1 cm DBH constitute the first census of the LFDP.

A second census of the entire plot was conducted between November 1994 and October 1996, during which period all trees ≥1 cm DBH were surveyed. During this second census, no damage was recorded, but all stems ≥1 cm DBH were scored for status (S), which was coded as dead ($S = 0$) or living ($S = 1$). Data from the first and second censuses allow us to explore the species-specific effects of hurricane damage, tree size, and degree of crowding on tree survival following Hurricane Hugo. Note that trees that were completely leafless and showing signs of rot during the first census were considered dead and excluded from the analysis. Thus, our analysis focuses on the effects of damage on tree survival during the hurricane recovery phase and does not address the immediate mortality caused by severe winds during the hurricane (Walker 1995).

Explicit analysis of all species in the LFDP is challenging because the site contains 89 species of trees with stems ≥10 cm DBH distributed in 72 genera and 38 families (Thompson et al. 2002). Of the 89 species in the LFDP 45 are rare (<1 stem/ha with DBH ≥ 10 cm), and over 75% of species have fewer than 5 stems/ha. For the purpose of this study, we limit our analysis to four species in the LFDP (see Table 6.1): the relatively shade-intolerant

Table 6.1 Species abundance and ecological characteristics. An index of shade tolerance is based on stems ≤10 cm DBH that experienced little or no hurricane damage and is given by the percentage of these stems that survived during canopy closure in the 2.5–5 year census periods following Hurricane Hugo. Hurricane susceptibility is the percentage of stems ≥10 cm DBH that were damaged in Hurricane Hugo. Wood density compiled from Brown (1997); successional status from Uriarte et al. (2004) and Thompson et al. (2002)

Species (Family)	No. of stems	Shade tolerance (%)	Hurricane susceptibility (%)	Wood density (g/cm^3)	Successional status
Casearia arborea (Flacourtiaceae)	5406	72.7	30.64	0.53	Secondary
Alchornea latifolia (Euphorbiaceae)	1130	49.7	33.26	0.39	Secondary
Dacryodes excelsa (Bursereaceae)	1490	96.7	0.05	0.57	Late
Manilkara bidentata (Sapotaceae)	1516	95.3	10.8	0.82	Late

fast growing species *Alchornea latifolia* and *Casearia arborea*, and the shade-tolerant species *Dacryodes excelsa* and *Manilkara bidentata*. These species are of particular interest because they are abundant in the LFDP and they represent a range of life histories and structural traits (e.g. Table 6.1). Thus, they are expected to differ in their susceptibility to hurricanes and subsequent mortality patterns (Zimmerman et al. 1994).

6.3   Statistical Models

Two primary objectives of this paper are (1) to evaluate species-specific susceptibility to hurricane damage and the implications for long-term survival, and (2) to illustrate the model building process for analyzing relatively complicated, hierarchically structured ecological data. We have chosen a Bayesian approach, but a comparable non-Bayesian likelihood analysis could have been employed, as was conducted for quantifying susceptibility of North American tree species to wind disturbance (e.g. Canham et al. 2001) (but this study did not analyze both damage *and* survival). Given that we use relatively noninformative priors and hyperpriors (described later in this section), we expect likelihood-based and Bayesian estimates to be similar (Gelman et al. 2004), but the simultaneous analysis of the damage (*D*) and survival (*S*) data is not easily accommodated by popular likelihood-based software. The Bayesian analysis, however, is easy to program in WinBUGS, and the posterior results are remarkably straightforward to interpret (e.g. Clark 2005; Gelfand and Clark, Chapter).

In the remainder of this section we focus on the model-building aspect of our objectives. We begin by developing the Bayesian model for a single species (Model 1) to establish the basic formulation for simultaneously estimating: (1) associations between tree size and hurricane damage, (2) effects of different degrees of damage on survival, and (3) the importance of tree size and crowding to survival. Model 1 simply serves as the building block for the hierarchical models (i.e. Model 2 and Model 3). For example, Model 2 extends Model 1 to multiple species, and Model 3 extends Model 2 to include random spatial (quadrat) effects. Model 2 and Model 3

are compared to determine which of these models is preferred, yielding insight into whether tree-level hurricane damage is spatially correlated after having accounted for species differences in size structure and susceptibility to wind disturbance.

6.3.1   Model 1: single species

Below we describe the single-species model (Model 1) in terms of the likelihood function for the survival and damage data and the posterior and prior probability densities for the model parameters. (For illustration purposes, we apply Model 1 to the data collected for *Casearia arborea*, but Model 1 could be easily implemented for all four species considered here.)

6.3.1.1   Likelihood
We decompose the joint likelihood for damage (*D*) and survival (or "status") (*S*) into a marginal likelihood for *D* multiplied by a conditional likelihood for *S* given *D*. For individual tree *i*, the likelihood function is given by:

$$L(D_i, S_i | \boldsymbol{\alpha}, \boldsymbol{\beta}, \text{DBH}_i, \text{BA}_i)$$
$$= L(D_i | \boldsymbol{\alpha}, \text{DBH}_i) L(S_i | \boldsymbol{\beta}, D_i, \text{DBH}_i, \text{BA}_i). \quad (6.1)$$

DBH_i (cm) is the stem diameter of tree i. BA_i (unitless, m^2/m^2) is a crowding index that is defined as the total basal area of all stems within a 15 m radius of the target tree (tree i) divided by the area of the neighborhood ($\pi \cdot 15^2$); we chose a 15 m radius because Uriarte et al. (2004) found that in the LFDP, trees outside of this range are unlikely to affect growth and survival of the target tree. The parameter vector $\boldsymbol{\alpha} = (\alpha_1, \alpha_2, \alpha_3 \, \alpha_4)$ defines the relationship between DBH and the probability of a tree experiencing no, medium, or heavy damage, and the parameter vector $\boldsymbol{\beta} = \beta_1, \beta_2, \beta_3, \beta_4, \beta_5)$ relates the probability of *remaining* alive between surveys to tree size, crowding, and the level (category) of damage suffered during the hurricane. Equations (6.3) and (6.5) and associated text give more detailed biological interpretation of $\boldsymbol{\alpha}$ and $\boldsymbol{\beta}$.

The marginal likelihood for damage is given by a multinomial distribution. Rather than using the original ordinate notation for *D* (i.e. $D = 0, 1,$ or 2), we switch to vector notation because it is more

appropriate for the multinomial representation; thus $D_i = 0$ is equivalent to $D_i = (1, 0, 0)$, $D_i = 1 = (0, 1, 0)$, and $D_i = 2 = (0, 0, 1)$, hence:

$$D_i \sim \text{Multin}(n, p_{0i}, p_{1i}, p_{2i} | \boldsymbol{\alpha}, \text{DBH}_i). \qquad (6.2)$$

Here, $n = 1$ because D_i is the observed damage vector for an *individual* tree. We assume that a tree's susceptibility to wind damage depends on its size (or DBH); in preliminary analyses we had also included BA as a covariate to reflect neighborhood effects (e.g. Harrington and DeBell 1996), but in all cases, BA was not a significant predictor of damage risk. Thus, the following baseline-category logits model (Agresti 2002) is employed for the damage probabilities:

$$
\begin{aligned}
\ln\left(\frac{p_{0i}}{p_{2i}}\right) &= \alpha_1 + \alpha_2 \cdot \frac{\text{DBH}_i}{100}, \\
\ln\left(\frac{p_{1i}}{p_{2i}}\right) &= \alpha_3 + \alpha_4 \cdot \frac{\text{DBH}_i}{100},
\end{aligned}
\qquad (6.3)
$$

where $\ln(\cdot)$ is the natural logarithm, and p_{0i}, p_{1i}, and p_{2i} are the prehurricane probabilities that tree i would have experienced no or little, intermediate, and severe damage, respectively ($p_{0i} + p_{1i} + p_{2i} = 1$). Although trees ≤ 10 cm DBH were scored for survival during the second census, they were not assessed for damage in the first census because many (but not all) of these trees were recruited into the forest *after* Hurricane Hugo. The exact timing of sapling establishment for each tree ≤ 10 cm is unknown. Hence, the damage data for these small trees were treated as "missing" or latent, but the Bayesian analysis provides posterior distributions for the latent damage variables. While these posteriors are essential for linking damage and survival probabilities of smaller trees, we are not directly interested in the latent damage variables, and thus we do not consider them any further.

The conditional likelihood for survival is described by a Bernoulli distribution. First, recall that $S_i = 0$ if tree i died between the first and second census, and $S_i = 1$ if it was still living when measured a second time. Thus, the conditional likelihood for survival is:

$$S_i \sim \text{Bern}(p_{T_i} | \boldsymbol{\beta}, D_i, \text{DBH}_i, \text{BA}_i), \qquad (6.4)$$

where p_{T_i} is the probability of tree i surviving the entire intercensus period, which depends on p_{S_i}, the probability of surviving from one year to the next. Although p_{S_i} may depend on time since Hurricane

Hugo (Walker 1995), we assume that p_{S_i} is time invariant because mortality rates tend to plateau by year three (Walker 1995). Status (*S*) was assessed 5–7 years after Hurricane Hugo, hampering our ability to estimate changes in p_{S_i} during the first 2–3 years. Hence, to account for variation in census length among trees, we assume that $p_{T_i} = (p_{S_i})^{T_i}$, where T_i is the number of years between the first and second census of tree i.

We assume that survival depends on damage, tree size, and crowding (e.g. Zimmerman et al. 1994; Walker 1995; Cooper-Ellis et al. 1999; Uriarte et al. 2004), which is captured in the logit model for p_{S_i}:

$$
\begin{aligned}
\ln\left(\frac{p_{S_i}}{1 - p_{S_i}}\right) &= \beta_1 \cdot \frac{\text{DBH}_i}{100} + \beta_2 \cdot 100 \cdot \text{BA}_i \\
&\quad + \beta_3 \cdot D_i(1) + \beta_4 \cdot D_i(2) \\
&\quad + \beta_5 \cdot D_i(3).
\end{aligned}
\qquad (6.5)
$$

$D_i(r)$ denotes the rth element of D_i, for example, if tree i was classified as undamaged, then $D_i = (1, 0, 0)$ and $D_i(1) = 1$, $D_i(2) = 0$, and $D_i(3) = 0$. In other words, $D_i(r)$ is a "dummy variable" for each damage class. The constants $1/100$ and 100 rescale DBH and BA, respectively, so that both predictor variables span a range of values between zero and one. The parameter β_1 captures the effect of size on survival, β_2 the effect of crowding, and β_3, β_4, and β_5 the effects of different levels of damage. The damage effects are most meaningful when compared to the undamaged condition. For example, $\beta_5 - \beta_3$ is the effect of being severely damaged (relative to not being damaged) on subsequent survival, and $\beta_4 - \beta_3$ is the (relative) effect of intermediate damage. We are most interested in evaluating these relative effects (versus direct evaluation of β_3, β_4, and β_5) because they explicitly quantify the effects of hurricane damage on subsequent survival.

6.3.1.2 *Posterior*

The goal of this analysis is to estimate the posterior density of the model parameters ($\boldsymbol{\alpha}$ and $\boldsymbol{\beta}$), thereby quantifying the strength and uncertainty in the linkages between hurricane-induced damage, survival, tree size, and crowding. The joint posterior density for $\boldsymbol{\alpha}$ and $\boldsymbol{\beta}$ is proportional to the likelihood

(for all trees) multiplied by the prior:

$$P(\boldsymbol{\alpha}, \boldsymbol{\beta}|\mathbf{D}, \mathbf{S}, \mathrm{DBH}, \mathbf{BA})$$

$$\propto \left(\prod_{i=1}^{N} L(D_i, S_i|\boldsymbol{\alpha}, \boldsymbol{\beta}, \mathrm{DBH}_i, \mathrm{BA}_i) \right) \pi(\boldsymbol{\alpha}, \boldsymbol{\beta}),$$

(6.6)

D, S, DBH, and BA are the data arrays for all trees, N is the total number of trees, and $\pi(\boldsymbol{\alpha}, \boldsymbol{\beta})$ is the prior density function for $\boldsymbol{\alpha}$ and $\boldsymbol{\beta}$ (see equation (6.7)).

6.3.1.3 Priors
Since no explicit information is available on the distribution of possible values for $\boldsymbol{\alpha}$ and $\boldsymbol{\beta}$, we choose relatively noninformative priors to complete equation (6.6). The prior density $\pi(\boldsymbol{\alpha}, \boldsymbol{\beta})$ is described by independent normal priors for $\boldsymbol{\alpha}$ and $\boldsymbol{\beta}$:

$$\boldsymbol{\alpha} \sim \mathbf{No}(\mathbf{0}, 100 \cdot \mathbf{I}), \qquad \boldsymbol{\beta} \sim \mathbf{No}(\mathbf{0}, 100 \cdot \mathbf{I}). \quad (6.7)$$

The prior variances are obtained by the following logic. First note that $p = \exp(u)/[1 + \exp(u)]$ if $\mathrm{logit}(p) = \ln[p/(1 - p)] = u$ (i.e. a logit model for a probability parameter p). Thus, in our logit models for damage and survival, $\boldsymbol{\alpha}$ and $\boldsymbol{\beta}$ enter into exponential functions. Note also that if $u \leq -10$ or $u \geq 10$, then $p \cong 0$ and $p \cong 1$, respectively. Additionally, for extreme values of u (e.g. $u < -100$ or $u > 100$), the evaluation of $\exp(u)$ could potentially lead to numerical overflow errors in the Markov chain Monte Carlo (MCMC) simulations (see Section 6.3.4 **Model Implementation**). Hence, we solved for σ^2, a prior variance, such that $10/\max(|X|) \leq 3 \cdot \sigma \leq 100/\max(|X|)$, where X is the predictor variable associated with a given parameter. This ensures that quantities in the logit equations, for example, $\alpha_1 \cdot \mathrm{DBH}/100$ and $\beta_2 \cdot 100 \cdot \mathrm{BA}$, rarely take on values outside of the interval $(-100, 100)$. The predictor variables X (i.e. DBH/100, $100 \cdot$ BA, and the damage dummy variables) have $\max(|X|)$ equal to or slightly less than one, thus all prior variances were set to 100.

6.3.2 Model 2: multiple species

We now extend Model 1 to a hierarchical model for multiple species (Model 2) and apply it to the four species in Table 6.1. This hierarchical extension is particularly easy to represent in a Bayesian

framework. The likelihood, posterior, and prior specifications for Model 2 follow the general scheme as outlined for Model 1, but an additional level that accounts for variation among multiple species and a set of hyperpriors is introduced. In the hierarchical model, there is a first-stage prior (very similar to the prior in Model 1) that describes the species-specific distributions from which individual tree parameters arise. A hyperprior (or second-stage prior) is also added that defines a "global" distribution from which the species-specific parameters arise.

6.3.2.1 Likelihood
The likelihood function is very similar to that in Model 1 such that for individual tree i, belonging to species j, the likelihood function is:

$$L(D_{ij}, S_{ij}|\boldsymbol{\alpha}_j, \boldsymbol{\beta}_j, \mathrm{DBH}_i, \mathrm{BA}_i)$$

$$= L(D_{ij}|\boldsymbol{\alpha}_j, \mathrm{DBH}_i)L(S_{ij}|\boldsymbol{\beta}_j, D_{ij}, \mathrm{DBH}_i, \mathrm{BA}_i).$$

(6.8)

Similar to Model 1, the marginal likelihood for damage is given by:

$$D_{ij} \sim \mathrm{Multin}(n, p_{0ij}, p_{1ij}, p_{2ij}|\boldsymbol{\alpha}_j, \mathrm{DBH}_i). \quad (6.9)$$

As before, $n = 1$ and the baseline logits model for the species-specific damage probabilities is:

$$\ln\left(\frac{p_{0ij}}{p_{2ij}}\right) = \alpha_{1j} + \alpha_{2j} \cdot \frac{\mathrm{DBH}_i}{100},$$

$$\ln\left(\frac{p_{1ij}}{p_{2ij}}\right) = \alpha_{3j} + \alpha_{4j} \cdot \frac{\mathrm{DBH}_i}{100}.$$

(6.10)

Similarly, the conditional likelihood for survival and the corresponding logit model for the probability of survival are given by:

$$S_{ij} \sim \mathrm{Bern}(p_{\mathrm{T}ij}|\boldsymbol{\beta}_j, D_{ij}, \mathrm{DBH}_i, \mathrm{BA}_i), \quad (6.11)$$

$$\ln\left(\frac{p_{\mathrm{S}ij}}{1 - p_{\mathrm{S}ij}}\right) = \beta_{1j} \cdot \frac{\mathrm{DBH}_i}{100} + \beta_{2j} \cdot 100 \cdot \mathrm{BA}_i$$

$$+ \beta_{3j} \cdot D_{ij}(1) + \beta_{4j} \cdot D_{ij}(2) + \beta_{5j} \cdot D_{ij}(3).$$

(6.12)

The complete likelihood formulation is essentially the same as for Model 1, with the main difference being that $\boldsymbol{\alpha}$ and $\boldsymbol{\beta}$ are indexed by the subscript j, indicating that the elements in these parameter vectors depend on species identity.

6.3.2.2 Posterior

Differences between Model 1 and Model 2 are more evident in the posterior, which clearly shows the hierarchical property of Model 2. Hence, the joint posterior density for the α_j's, β_j's, and γ (i.e. a set of hyperparameters associated with the hyperprior) is proportional to the likelihood multiplied by the first-stage prior and hyperprior:

$$P(\alpha_1, \ldots, \alpha_J, \beta_1, \ldots, \beta_J, \gamma | \mathbf{D}, \mathbf{S}, \mathbf{DBH}, \mathbf{BA})$$

$$\propto \left(\prod_{j=1}^{J} \prod_{i=1}^{N_j} L(D_{ij}, S_{ij} | \alpha_j, \beta_j, \gamma, \mathrm{DBH}_i, \mathrm{BA}_i) \right)$$

$$\times \pi(\alpha_1, \ldots, \alpha_J, \beta_1, \ldots, \beta_J | \gamma) \cdot \pi(\gamma), \qquad (6.13)$$

where J is the total number of species, and N_j is the number of trees identified as species j. The prior component differs from Model 1 in that the first-stage prior for the α_j's and β_j's is conditioned on $\gamma = (\mu_\alpha, \mu_\beta, \sigma_\alpha, \sigma_\beta)$ and a hyperprior for γ is introduced.

6.3.2.3 Priors and hyperpriors

We again use normal probability densities for the priors, and $\pi(\alpha_1, \ldots, \alpha_J, \beta_1, \ldots, \beta_J | \gamma)$ is broken-up into nine independent first-stage priors, one for each of the four α_j (equation (6.10)) and five β_j (equation (6.12)) elements:

$$\alpha_{1j} \sim \mathrm{No}(\mu_{\alpha 1}, \sigma_{\alpha 1}^2), \ldots, \alpha_{4j} \sim \mathrm{No}(\mu_{\alpha 4}, \sigma_{\alpha 4}^2),$$

$$\beta_{1j} \sim \mathrm{No}(\mu_{\beta 1}, \sigma_{\beta 1}^2), \ldots, \beta_{5j} \sim \mathrm{No}(\mu_{\beta 5}, \sigma_{\beta 5}^2).$$

$$(6.14)$$

Likewise, $\pi(\gamma)$ is also decomposed into 18 independent hyperpriors, one for each of the four μ_α, five μ_β, four σ_α, and five σ_β elements of γ as shown in equation (6.14). Independent normal densities are used for μ_α and μ_β, and independent gamma densities are employed for the precisions $v_{\alpha 1} = 1/\sigma_{\alpha 1}^2, \ldots, v_{\alpha 4} = 1/\sigma_{\alpha 4}^2$ and $v_{\beta 1} = 1/\sigma_{\beta 1}^2, \ldots, v_{\beta 5} = 1/\sigma_{\beta 5}^2$:

$$\mu_\alpha \sim \mathrm{No}(0, 100 \cdot \mathbf{I}),$$

$$\mu_\beta \sim \mathrm{No}(0, 100 \cdot \mathbf{I}),$$

$$v_{\alpha 1} \sim \mathrm{Ga}(0.5, 2), \ldots, v_{\alpha 4} \sim \mathrm{Ga}(0.5, 2),$$

$$v_{\beta 1} \sim \mathrm{Ga}(0.5, 2), \ldots, v_{\beta 5} \sim \mathrm{Ga}(0.5, 2).$$

$$(6.15)$$

Equation (6.15) gives relatively noninformative hyperpriors, which were derived by the same logic that was used to define the priors in Model 1. Note that the gamma density is parameterized such that if $y \sim \mathrm{Ga}(a, b)$ then $E(y) = a/b$ and $\mathrm{Var}(y) = a \cdot (a + 1)/(b^2)$.

6.3.3 Model 3: multiple species with spatial process

Finally, we extend Model 2 to include a spatial process that captures quadrat-to-quadrat autocorrelation in hurricane intensity, yielding Model 3. Such spatial variation is potentially driven by several larger scale factors such as the trajectory of the storm, distance to the eye of the storm, topography, and land-use history, but we do not explicitly model these effects in this study. Rather, we begin with a fairly simple spatial model that allows us to quantify the degree of spatial pattern in hurricane damage.

6.3.3.1 Likelihood

The LFDP dataset contains damage assessments for trees in all 400 (20 m × 20 m) quadrats that make up the plot. We modify the marginal damage likelihood to reflect quadrat-specific random effects. This spatial error structure is described by an intrinsic Gaussian conditional autoregressive (CAR) model (see Banerjee et al. 2004, and references within), which captures the spatial autocorrelation among adjacent quadrats. Thus, for individual tree i, belonging to species j, and growing in quadrat k, the likelihood function is:

$$L(D_{ijk}, S_{ijk} | \alpha_j, \beta_j, \varphi_k, \mathrm{DBH}_i, \mathrm{BA}_i)$$

$$= L(D_{ijk} | \alpha_j, \varphi_k, \mathrm{DBH}_i)$$

$$\times L(S_{ijk} | \beta_j, D_{ijk}, \mathrm{DBH}_i, \mathrm{BA}_i). \qquad (6.16)$$

Equation (6.16) differs from Equation (6.18) by the inclusion of $\varphi_k = (\varphi_{1k}, \varphi_{2k})$, which represents the spatial residuals in hurricane damage (see equations (6.18) and (6.20)). The marginal likelihood for damage is:

$$D_{ijk} \sim \mathrm{Mulitn}(n, p_{0ijk}, p_{1ijk}, p_{2ijk} | \alpha_j, \mathrm{DBH}_i, \varphi_k). \qquad (6.17)$$

The damage probabilities explicitly depend on location (quadrat) because the CAR terms are directly

incorporated into the baseline category logits model:

$$\ln\left(\frac{p_{0ijk}}{p_{2ijk}}\right) = \alpha_{1j} + \alpha_{2j} \cdot \frac{\text{DBH}_i}{100} + \varphi_{1k},$$

$$\ln\left(\frac{p_{1ijk}}{p_{2ijk}}\right) = \alpha_{3j} + \alpha_{4j} \cdot \frac{\text{DBH}_i}{100} + \varphi_{2k}.$$

(6.18)

With the exception of an added k subscript, the conditional likelihood for survival and the logit model for the probability of survival are the same as for Model 2 (equations (6.11) and (6.12)).

6.3.3.2 *Posterior*

The joint posterior density for the α_j's, β_j's, φ_k's, γ, and τ (a hyperparameter set for the CAR model) is modified from Model 2 as:

$$P(\alpha_1, \ldots, \alpha_J, \beta_1, \ldots, \beta_J, \varphi_1, \ldots,$$

$$\varphi_Q, \gamma, \tau | \mathbf{D}, \mathbf{S}, \mathbf{DBH}, \mathbf{BA})$$

$$\propto \left(\prod_{k=1}^{Q}\prod_{j=1}^{J}\prod_{i=1}^{N_{jk}} L(D_{ijk}, S_{ijk} | \alpha_j, \beta_j, \varphi_k,\right.$$

$$\left.\text{DBH}_i, \text{BA}_i)\right)$$

$$\times \pi(\alpha_1, \ldots, \alpha_J, \beta_1, \ldots, \beta_J | \gamma)$$

$$\times \pi(\varphi_1, \ldots, \varphi_Q | \tau) \cdot \pi(\gamma) \cdot \pi(\tau), \qquad (6.19)$$

where Q is the total number of quadrats, and N_{jk} is the number of trees of species j in quadrat k. The conditional autoregressive property of the model is seen in the first-stage prior specification for the φ_k's, which assumes that the spatial residual for damage in quadrat k depends in part on the residuals of neighboring plots ($m \neq k$), as described below.

6.3.3.3 *Priors and hyperpriors*

Partitioning the spatial random effects into two parts (versus one) allows us to capture spatial correlation in all three damage categories. We use a relatively simple model where the first-stage prior probability density for the spatial random effect φ_k is partitioned into the two independent Gaussian CAR models for φ_{1k} and φ_{2k}:

$$\varphi_{1k}|\varphi_{1m} \sim \text{No}\left(\frac{1}{\omega_{k+}} \cdot \sum_{m \in \delta_k} \omega_{km} \cdot \varphi_{1m}, \frac{1}{\omega_{k+} \cdot \tau_1}\right),$$

$$\varphi_{2k}|\varphi_{2m} \sim \text{No}\left(\frac{1}{\omega_{k+}} \cdot \sum_{m \in \delta_k} \omega_{km} \cdot \varphi_{2m}, \frac{1}{\omega_{k+} \cdot \tau_2}\right),$$

$$\omega_{k+} = \sum_{m \in \delta_k} \omega_{km},$$

(6.20)

where δ_k is a set of neighboring quadrats associated with quadrat k, and quadrat k itself is not included in the set. In our analysis, neighboring quadrats that share an edge or a diagonal corner with quadrat k are included in δ_k. The relative "importance" of neighboring quadrat m to the residual of quadrat k is captured by the weight ω_{km} (we assume equal weights such that $\omega_{km} = 1$ for all k and m). Thus, the total number of neighbor quadrats associated with quadrat k is $\omega_{k+} = 3$ if quadrat k is one of four corner quadrats, $\omega_{k+} = 5$ if quadrat k is along the edge of the LFDP, and $\omega_{k+} = 8$ if quadrat k is located within the plot interior.

The hyperprior $\pi(\tau)$ for the CAR precision parameters $\tau = (\tau_1, \tau_2)$ (equation (6.20)) is split into two independent gamma densities for τ_1 and τ_2:

$$\tau_1 \sim \text{Ga}(0.5, 2), \qquad \tau_2 \sim \text{Ga}(0.5, 2). \qquad (6.21)$$

Finally, we use the same specification for $\pi(\alpha_1, \ldots, \alpha_J, \beta_1, \ldots, \beta_J | \gamma)$ and $\pi(\gamma)$ is given in Model 2, equations (6.14) and (6.15), respectively.

6.3.4 Model implementation

The nonlinear nature of the likelihood functions makes it difficult to obtain analytical solutions for the posterior densities. Thus, we employed MCMC simulation techniques to generate samples from the posteriors (see Gilks et al. 1996). We programmed the three models in WinBUGS, which is the MS Windows version of the BUGS (*B*ayesians *U*sing *G*ibbs *S*ampling) software package (WinBUGS documentation and software can be downloaded at http://www.mrc-bsu. cam.ac.uk/bugs/welcome.shtml). For each model, we ran three parallel MCMC chains for 79,000 iterations. Starting values for each chain were generated

from "tighter" versions of the prior and hyperprior densities. We used the "bgr" diagnostics tool in WinBUGS, which is based on Gelman and Rubin (1992) and Books and Gelman (1998), to monitor convergence of the chains to a stationary posterior distribution. All chains converged by iteration 4000, hence we used iterations 4001 to 79,000, and we kept every 60th sample from each chain to provide independent samples from the posterior of size 3750. Thus, with probability 0.95 the empirical 0.025, 0.50, and 0.975 quantiles are expected to provide estimates of the 0.025 ± 0.005, 0.50 ± 0.016, and 0.975 ± 0.005 posterior quantiles, respectively (e.g. Raftery and Lewis 1996).

6.3.5 Model comparisons and selection

For pedagogical purposes, we compare Models 1, 2, and 3 to examine the effects of different model specifications on the posterior estimates of the parameters that determine the probabilities of damage and survival (α and β, respectively). Here, this comparison is only relevant to *C. arborea* because it is the only species considered in all three models. Two models may be considered to yield similar parameter estimates if each parameter's posterior mean under one model is contained within the respective parameter's central 95% credible interval (CrI) of the other model. We also employ a stricter criterion whereby models are considered to yield dissimilar estimates if the 95% CrIs of their corresponding parameters do not overlap.

More rigorous comparisons between Model 2 and Model 3 (but not Model 1) are conducted for all four species. Again, posterior means and CrIs for the α and β parameters are compared between Model 2 and Model 3. A formal evaluation is also employed by calculating the deviance (-2 log likelihood) and deviance information criteria (DIC) (Spiegelhalter et al. 2002). DIC provides a measure of model fit, penalized by the effective number of parameters, and the model with the smallest DIC is preferred (Spiegelhalter et al. 2002). While DIC is a useful model selection tool, it gives a single number per model, and thus provides limited insight into model behavior. Hence, we also conducted an informal goodness-of-fit assessment to compare Model 2 and Model 3 with respect to their abilities to capture the observed variation in survival and damage. First we obtained estimates of each tree's posterior probabilities of survival (p_T) and of experiencing little (p_0), moderate (p_1), or severe damage (p_2). That is, we calculated a p_T, p_0, p_1, and p_2 value for each tree based on its size (DBH), crowding index (BA), the species-specific posterior means for α_j and β_j, and, for Model 3, the posterior means for the quadrat effects (φ_{1k} and φ_{2k}). We then grouped trees by their predicted p_T and p_0 values, calculated the observed damage and survival rates of each group, and compared the observed estimates to the average predicted p_T and p_0 value of each group. Predictions and observations are in close agreement if the observed versus predicted p_T and p_0 values fall along the 1:1 line.

6.4 Results

6.4.1 Model comparisons and selection

We first compared Models 1, 2, and 3 with respect to their posterior estimates of α and β given for *C. arborea* (see Table 6.2 for *C. arborea*'s posterior means and 95% CrI's). The α and β estimates given by Model 1 and Model 2 are nearly identical: the 95% CrI's for each parameter overlap and the posterior mean of each parameter under one model is contained within the respective parameter's 95% CrI of the other model (Table 6.2). The addition of the CAR specification (Model 3) had little effect on the estimates of the survival parameters (β's) (Table 6.2). However, based on comparing *posterior means* (Model 3) to *posterior CrI's* (Models 1 and 2), Model 3 appears to result in slightly different estimates for the damage parameters (α's): the posterior means for $\alpha_1, \alpha_2, \alpha_3$, and α_4 associated with Model 3 often fall outside of the 95% CrI's given by other two models (Table 6.2). If we evaluate whether or not CrI's overlap, then it appears that the α estimates do not differ radically between the three models because the 95% CrI's for the α's in Model 3 overlap with the 95% CrI's given by Model 1 and Model 2 (with the exception of α_1 from Model 3 versus Model 1, Table 6.2).

Model 2 and Model 3 are more appropriate for investigating species-specific responses to hurricane disturbance because they can accommodate multiple species (see Table 6.3 for their species-specific

Table 6.2 Posterior means and central 95% credible intervals (in parentheses) for the hurricane damage and survival parameters for *C. arborea* under the three different models

Parameter	Model 1	Model 2	Model 3
Parameter estimates for log odds of no damage versus severe damage: $\ln(p_0/p_2) = \alpha_1 + \alpha_2 \cdot (DBH/100)$			
α_1	2.076	1.847	1.231
	(1.446, 2.694)	(1.229, 2.481)	(0.866, 1.631)
α_2	−7.032	−5.738	−1.293
	(−10.470, −3.539)	(−9.192, −2.308)	(−3.427, 0.687)
Parameter estimates for log odds of moderate damage versus severe damage: $\ln(p_1/p_2) = \alpha_3 + \alpha_4 \cdot (DBH/100)$			
α_3	−2.097	−2.040	−3.067
	(−2.868, −1.344)	(−2.696, −1.473)	(−3.827, −2.372)
α_4	4.904	4.725	8.526
	(1.385, 8.474)	(2.071, 7.820)	(5.523, 12.030)
Parameter estimates for logit of annual survival: $\ln(p_S/(1 - p_S)) = \beta_1 \cdot (DBH/100) + \beta_2 \cdot 100 \cdot BA + \beta_3 \cdot D(1) + \beta_4 \cdot D(2) + \beta_5 \cdot D(3)$			
β_1	3.760	3.452	2.466
	(2.461, 5.012)	(2.153, 4.722)	(1.263, 3.714)
β_2	1.635	1.598	1.954
	(0.923, 2.322)	(0.868, 2.316)	(1.187, 2.757)
β_3	1.728	1.802	2.059
	(1.445, 2.037)	(1.501, 2.124)	(1.736, 2.399)
β_4	1.163	1.263	1.362
	(0.631, 1.709)	(0.724, 1.810)	(0.830, 1.934)
β_5	0.118	0.181	0.048
	(−0.255, 0.470)	(−0.183, 0.521)	(−0.308, 0.397)

posterior estimates of $\boldsymbol{\alpha}$ and $\boldsymbol{\beta}$). Comparisons of Model 2 and Model 3 provide information about the importance of spatially correlated damage risk. First, how does the addition of the CAR model affect the estimates of $\boldsymbol{\alpha}$ and $\boldsymbol{\beta}$? With the exception of α_{33} and α_{34} (the intercept in the log-odds of intermediate versus severe damage for *D. excelsa* and *M. bidentata*, respectively; see equations (6.10) and (6.18)), the posterior means are consistent in that each parameter's mean maintains the same sign and magnitude between Model 2 and Model 3. Conversely, Model 2 suggests that if small trees (i.e. DBH $\cong$ 0) of *D. excelsa* and *M. bidentata* are exposed to hurricane disturbance then they are equally likely to be moderately or severely damaged (α_{33}, $\alpha_{34} \cong 0$), but Model 3 implies that they are more likely to suffer severe compared to moderate damage (α_{33}, $\alpha_{34} < 0$).

Second, differences in parameter estimates *among* species were generally comparable between Model 2 and Model 3 (Table 6.3). For instance, both models suggest that all species are similar with respect to

α_{4j} such that the log-odds of a tree suffering moderate versus severe damage significantly increases with tree size ($\alpha_{4j} > 0$ for all j; Table 6.3). Both models also suggest that the baseline survival rate (i.e. survival of an undamaged tree with DBH $\cong$ 0 and BA $\cong$ 0) is much lower for *C. arborea* and *A. latifolia* compared to *D. excelsa* and *M. bidentata* (i.e. $\beta_{41} \cong \beta_{42} < \beta_{43} \cong \beta_{44}$; Table 6.3). Inclusion of the CAR process, however, generally leads to wider interval estimates for the α's and narrower intervals for the β's. For example, under Model 2, the narrower CrIs for the α's are likely an artifact of incorrectly assuming that the damage data are spatially independent, thereby essentially overestimating the amount of information available to estimate $\boldsymbol{\alpha}$.

A formal evaluation based on DIC confirms that Model 3 (DIC = 9,807) is preferred over Model 2 (DIC = 10,391). The difference in DIC values of 584 is exceptionally large (Spiegelhalter et al. 2002), indicating that the data provide very little to no support for Model 2 compared to Model 3.

Table 6.3 Posterior means for the hurricane damage and survival parameters. Means are given for the four species (Table 6.1) based on Model 2 and Model 3. Within a row (or parameter), letters in parentheses indicate species differences (i.e. the central 95% credible intervals for pairwise differences do not contain zero). Parameters with parentheses followed by an asterisk differ from zero (i.e. the central 95% credible interval does not contain zero)

Parameter	Species			
	C. arborea ($j = 1$)	A. latifolia ($j = 2$)	D. excelsa ($j = 3$)	M. bidentata ($j = 4$)
Model 2: Multiple species				
α_{1j}	1.847 (ab)*	1.140 (a)*	2.526 (b)*	2.186 (b)*
α_{2j}	−5.738 (a)*	−0.128 (b)	−0.538 (b)	−1.740 (b)
α_{3j}	−2.040 (a)*	−0.795 (b)	0.389 (c)	0.286 (c)
α_{4j}	4.725 (a)*	4.397 (a)*	4.183 (a)*	3.883 (a)*
β_{1j}	3.452 (b)*	11.180 (c)*	−1.878 (a)	5.233 (b)*
β_{2j}	1.598 (b)*	−1.949 (a)*	5.262 (c)*	2.182 (bc)
β_{3j}	1.802 (a)*	2.268 (a)*	4.145 (b)*	3.805 (b)*
β_{4j}	1.263 (a)*	1.416 (a)*	3.767 (b)*	4.667 (b)*
β_{5j}	0.181 (a)	0.303 (a)	0.234 (a)	0.771 (a)
Model 3: Multiple species with spatial process				
α_{1j}	1.231 (a)*	1.262 (a)*	2.545 (b)*	2.247 (b)*
α_{2j}	−1.293 (a)	−0.240 (a)	−0.690 (a)	−1.619 (a)
α_{3j}	−3.067 (a)*	−1.399 (b)*	−1.082 (b)*	−1.146 (b)*
α_{4j}	8.526 (a)*	6.057 (a)*	5.954 (a)*	7.102 (a)*
β_{1j}	2.466 (b)*	10.760 (c)*	−2.056 (a)*	4.904 (b)*
β_{2j}	1.954 (b)*	−1.527 (a)*	5.055 (c)*	1.987 (bc)
β_{3j}	2.059 (a)*	2.180 (a)*	4.331 (b)*	3.842 (b)*
β_{4j}	1.362 (a)*	1.186 (a)*	3.921 (b)*	4.715 (b)*
β_{5j}	0.048 (a)	0.325 (a)	0.346 (a)	0.954 (a)

However, the DIC calculations resulted in negative values for the number of effective parameters. The conditions under which negative effective parameters are encountered and the consequences of such values are not clearly understood (see Spiegelhalter et al. 2002, and associated discussion papers); thus DIC must be used with caution in this study. The deviance values also suggest that Model 3 is strongly preferred over Model 2 (posterior mean of the deviance is 10,820 and 12,060 for Model 3 and Model 2, respectively).

We also conducted an informal model goodness-of-fit assessment (e.g. Figure 6.2) because DIC may not be appropriate for selecting between Model 2 and Model 3, and it lends little insight into model behavior. For both models, observed versus predicted values for the probabilities of experiencing little or no damage (p_0) and of surviving the census interval (p_T) fall along the 1:1 line for all species (Figure 6.2). It also appears that Model 2 and Model 3 are equally capable of capturing the observed variation in damage (compare Figure 6.2(a) versus Figure 6.2(b)) and survival (Figure 6.2(c) versus Figure 6.2(d)). Model 3, however, is preferred over Model 2 because the posterior estimates of the CAR precision parameters (τ_1 and τ_2) indicate that there is significant spatial autocorrelation in observed damage. For example, τ_1 and τ_2 are tightly clustered around their posterior means of 0.303 and 0.113, with 95% CrI's of [0.200, 0.447] and [0.076, 0.166], respectively. The posterior means for τ_1 and τ_2 give standard deviation estimates of 1.556 and 0.950 for interior quadrats ($\omega_{k+} = 8$), which are fairly large values given that they enter into the *log* odds equations for the baseline-logits model (equation (6.18)). Hence, both the formal and informal model comparisons indicate that the damage data are spatially correlated, therefore we
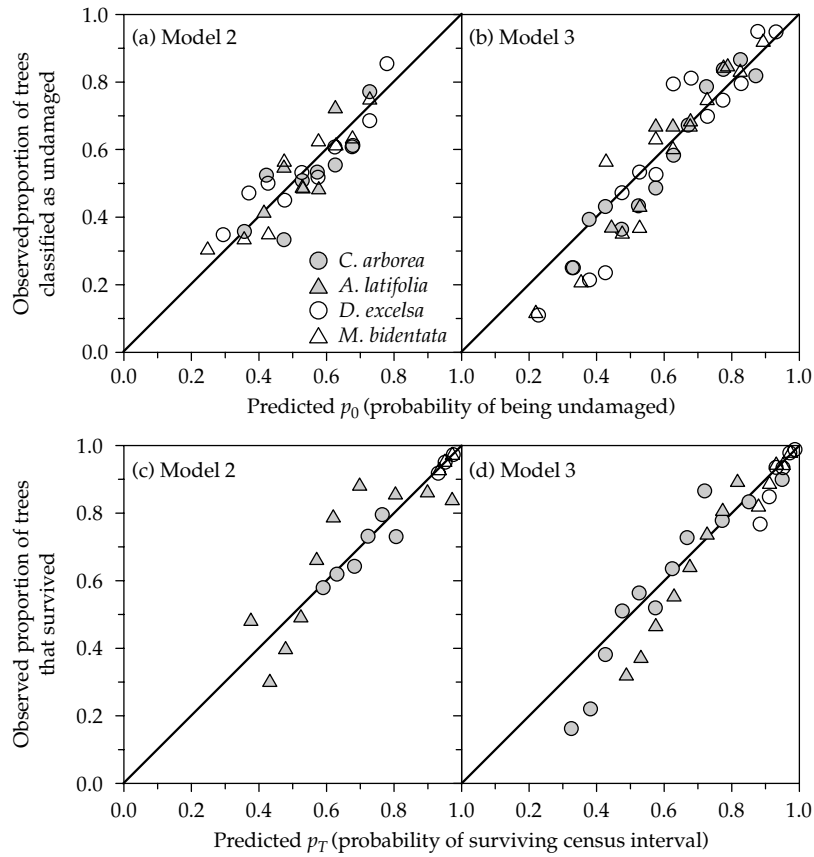
Figure 6.2. Assessment of model goodness-of-fit. The goodness-of-fit plot was derived according to the following steps. First, we calculated the posterior means for each species' damage and survival parameters (α_j and β_j, respectively) and for the quadrat effects (φ_{1k} and φ_{2k}) given by Model 2 and Model 3. Second, we obtained an estimate of the damage probabilities (p_0, p_1, and p_2) for each tree by substituting the posterior means for α_j, φ_{1k}, and φ_{2k} into equation (6.10) (Model 2) and equation (6.20) (Model 3). Third, we calculated each tree's probability of surviving its census interval conditional on its observed level of damage (i.e. calculated $p_{T|D}$). For each damage category d ($d = 0, 1, 2$), $p_{T|D=d}$ was calculated by substituting the β_j posterior means into equation (6.12), by setting $D_{ij}(r = d) = 1$ and D_{ij} ($r \neq d) = 0$, and by using the relationship $p_T = (p_S)^T$. Fourth, an estimate of each tree's total (i.e. marginal) probability of surviving is given by $p_T = p_{T|(D=0)} \cdot p_0 + p_{T|(D=1)} \cdot p_1 + p_{T|(D=2)} \cdot p_2$ (i.e. sum over the conditional probability of surviving multiplied by the corresponding damage probability). Fifth, within each species, trees were grouped according to their predicted p_0 value, with a fixed bin width of 0.05; within each p_0 bin, the fraction of trees classified as having no/little damage and the average value of p_0 was calculated, giving the observed fraction of trees with $D = 0$ versus the average predicted probability of having $D = 0$ for (a) Model 2 and (b) Model 3. Finally, within each species, trees were binned according to their p_T values, with fixed bin widths of 0.05 for *C. arborea* and *A. latifolia* and 0.02 for *D. excelsa* and *M. bidentata*. Within each bin, the mean observed survival rate versus the mean probability of surviving were calculated for (c) Model 2 and (d) Model 3.

focus on Model 3 for the remainder of the results section.

6.4.2 Multiple species with spatial process

6.4.2.1 Species-specific susceptibility to damage
The four species considered here appear to vary greatly with respect to their susceptibility to

hurricane damage (see α's, Model 3, Table 6.1). These differences are primarily captured by α_1 and α_3 (the intercepts of the log odds for no/little versus severe damage and for moderate versus severe damage, respectively, equation (6.10)). For example, the probability of suffering severe (relative to no/little) damage during a hurricane event is greater for *C. arborea* and *A. latifolia* compared to *D. excelsa*

and $M.\ bidentata$ (i.e. $\alpha_{11} \leq \alpha_{12} < \alpha_{14} \leq \alpha_{13}$), regardless of tree size (α_{2j} is similar among species). The nonlinear way in which $\boldsymbol{\alpha}$ affects the multinomial damage probabilities complicates its interpretation, but the combined effect of $\boldsymbol{\alpha}$ and DBH on the damage probabilities is shown in Figure 6.3. Across all species, the posterior mean for the probability of escaping damage (p_0) decreases monotonically with increasing tree size (Figure 6.3(a,d,g,j)), and the posterior mean for the probability of suffering

moderate damage (p_1) increases monotonically with increasing tree size (Figure 6.3(b,e,h,k)). In contrast, p_2 varies widely between species such that $C.\ arborea$ shows a near constant, but relatively high, probability of suffering severe damage (Figure 6.3(c)); p_2 is also high for $A.\ latifolia$, but it gradually decreases with increasing DBH (Figure 6.3(f)); $D.\ excelsa$ and $M.\ bidentata$ have very low probabilities of suffering severe damage over the whole range of tree sizes (Figure 6.3(i,l)).
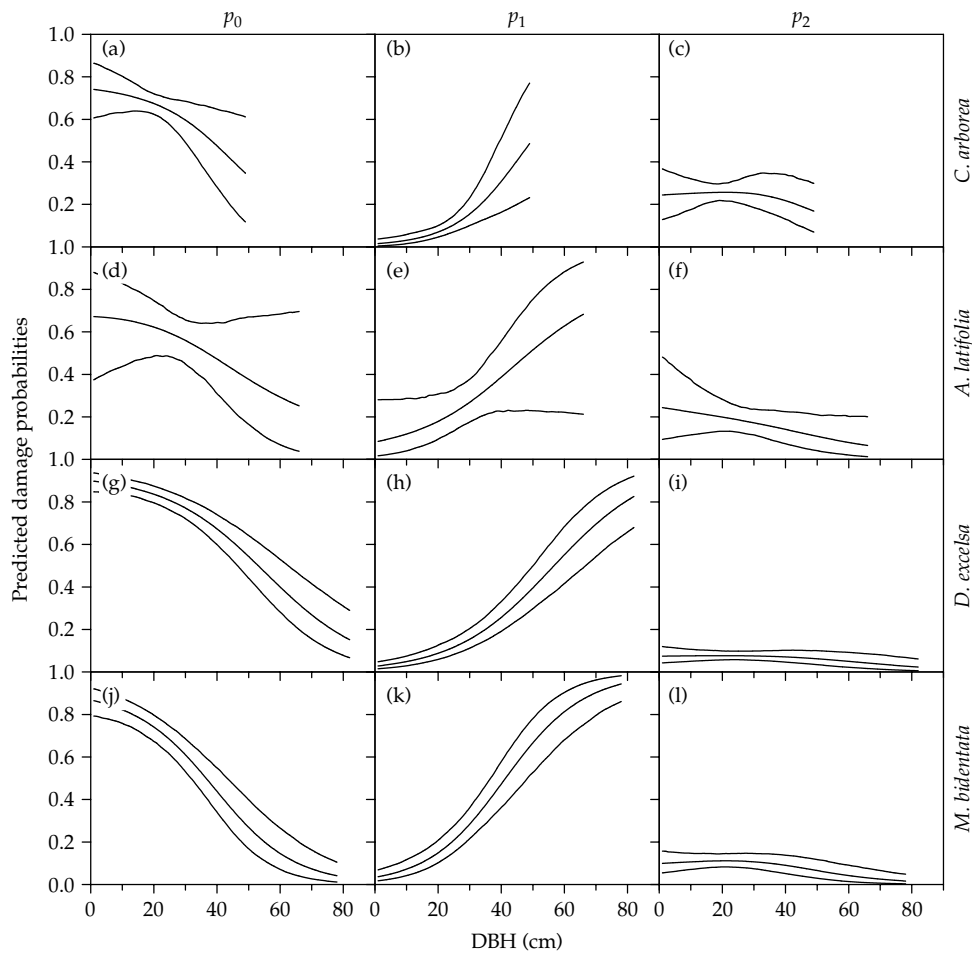
Figure 6.3. Predicted damage probabilities as a function of tree size (DBH). Each panel shows the curves representing the posterior mean and the 95% CrI for each damage probability based on the posterior samples for α_1, α_2, α_3, and α_4 under Model 3. Within a row, panels correspond to a given species; columns are, from right to left, the probabilities of experiencing no damage (p_0), moderate damage (p_1), and severe damage (p_2). The panels are: (a) p_0 for $Casearia\ arborea$, (b) p_1 for $C.\ arborea$, (c) p_2 for $C.\ arborea$, (d) p_0 for $Alchornea\ latifolia$, (e) p_1 for $A.\ latifolia$, (f) p_2 for $A.\ latifolia$, (g) p_0 for $Dacryodes\ excelsa$, (h) p_1 for $D.\ excelsa$, (i) p_2 for $D.\ excelsa$, (j) p_0 for $Manilkara\ bidentata$, (k) p_1 for $M.\ bidentata$, and (l) p_2 for $M.\ bidentata$. Curves span the DBH range observed for each species.
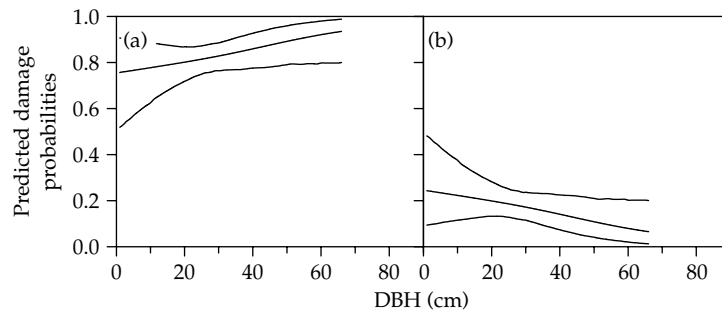
Figure 6.4. Predicted binomial damage probabilities as a function of DBH for *A. latifolia*. The three original damage categories were collapsed into two, giving curves for the posterior mean and 95% CrI for each binomial probability, where (a) is the probability of experiencing little or no damage (i.e. $p_0 + p_1$), and (b) is the probability of suffering severe damage (p_2), which is the same as Figure 6.3(f).

The level of uncertainty in the estimated damage probabilities varies among species. The two species identified as hurricane susceptible (*A. latifolia* and *C. arborea*) exhibit large variation in their predicted damage probabilities (see wide CrI's in Figure 6.3(a)–(f)). This is especially the case for *A. latifolia*, which has exceptionally wide intervals for p_0 and p_1. However, when these two damage categories are combined into one, then the CrI for $p_0 + p_1$ is considerably narrower than those for p_0 or p_1 alone (compare Figure 6.4(a) to Figure 6.3(d,e)). This potentially indicates that a binomial classification of low versus severe damage is sufficient for describing the damage to *A. latifolia* by hurricanes. The binomial estimates suggest that the level of damage incurred by *A. latifolia* is essentially independent of tree size (see nearly flat posterior means and CrI's in Figure 6.3(a,b)). In contrast to *A. latifolia* and *C. arborea*, the CrIs for the damage probabilities are exceptionally narrow for *D. excelsa* and *M. bidentata*. For these latter two species, the tight intervals imply a strong relationship between tree size and the probability of escaping damage (Figure 6.3(g,j)) or of suffering moderate damage (Figure 6.3(h,k)); the tight, flat interval for p_2 indicates that trees of all sizes are equally likely, but very unlikely, to suffer severe damage (Figure 6.3(i,l)).

6.4.2.2 Species-specific posthurricane survival
The four species clearly diverge with regard to survival following a hurricane. Their annual survival probabilities (p_S) differ in terms of correlations with tree size (DBH) (see β_{1j} in Table 6.3), effects of crowding (β_{2j}, Table 6.3), and the consequences of different degrees of damage for subsequent survival (β_{3j} and β_{4j}, Table 6.3). For *A. latifolia*, *C. arborea*, and *M. bidentata*, the probability of survival was higher for larger trees (β_{11}, β_{12}, $\beta_{14} > 0$) while the opposite was true for *D. excelsa* ($\beta_{13} < 0$). Survival of *C. arborea* and *D. excelsa* was impaired in low density stands (β_{21}, $\beta_{23} > 0$), the contrary was true for *A. latifolia* ($\beta_{22} < 0$), and survival of *M. bidentata* was not affected by basal area of neighbors ($\beta_{24} \cong 0$). The effect of hurricane damage on subsequent survival is more clearly demonstrated by comparing the effect of moderate or severe damage versus undamaged; that is, by evaluating $\beta_4 - \beta_3$ (moderate damage effect) and $\beta_5 - \beta_3$ (severe damage effect). Two patterns emerge when comparing these relative damage effects: (1) both moderate and severe damage consistently reduce survival of the hurricane-susceptible species such that the $\beta_4 - \beta_3$ and $\beta_5 - \beta_3$ estimates are less than zero for *C. arborea* and *A. latifolia* (Figure 6.5(a,b)); (2) moderate levels of damage had little effect on survival of the hurricane-resistant species, *D. excelsa* and *M. bidentata* (the posteriors for $\beta_4 - \beta_3$ contain zero), but their probabilities of survival were greatly reduced by severe damage (the posteriors for $\beta_5 - \beta_3$ are located to the far left of zero) (Figure 6.5(c,d)).

The tight marginal posteriors for the relative damage effects estimated for *C. arborea* clearly indicate that survival is differentially affected by the three levels of damage (Figure 6.5(a)). For *A. latifolia*, the overlapping posteriors for the relative damage effects suggest that both moderate
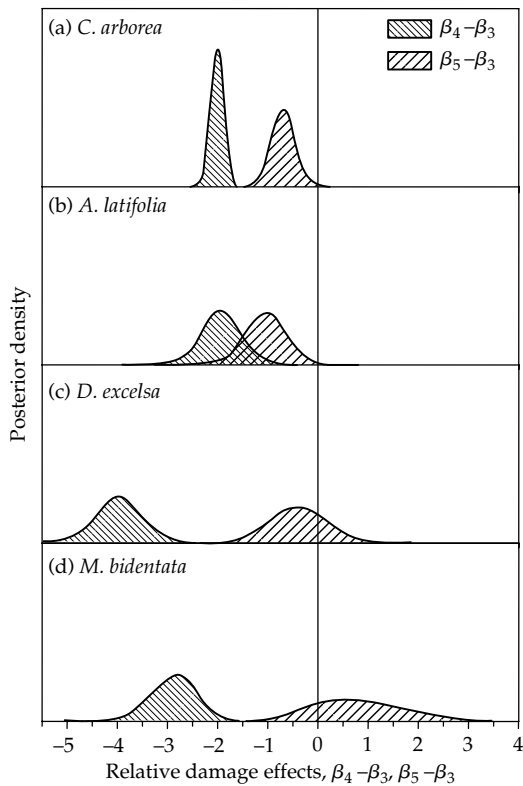
Figure 6.5. Posterior distributions describing the effect of damage on year-to-year survival rate (p_S) based on Model 3. The effect of moderate damage (relative to undamaged) is given by $\beta_4 - \beta_3$, and the effect of severe damage (relative to undamaged) is given by $\beta_5 - \beta_3$ for (a) *C. arborea* ($j = 1$), (b) *A. latifolia* ($j = 2$), (c) *D. excelsa* ($j = 3$), and (d) *M. bidentata* ($j = 4$). For example, if species j is characterized by a $\beta_5 - \beta_3$ effect that is *less than zero*, this implies that a tree of Species j experiencing severe damage is more likely to die (less likely to survive) than one experiencing little or no damage. The vertical line corresponds to zero (no effect of damage on survival).

and severe damage reduce survival to a similar degree (Figure 6.5(b)). The effect of severe damage on subsequent survival is similar for *A. latifolia*, *C. arborea*, and *M. bidentata*, but the negative effect of severe damage is particularly pronounced for *D. excelsa* (Figure 6.5(c)). Although the species differ somewhat in the extent to which severe damage effects survival (e.g. Figure 6.6(b)), the marginal posterior describing the variation *among* species (i.e. $\mu_{\beta5} - \mu_{\beta3}$) clearly indicates that severe hurricane damage decreases tree survivorship in the years following a storm (Figure 6.6(a)).
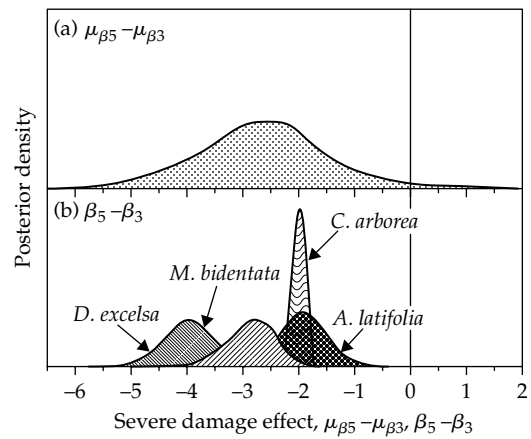

Figure 6.6. Posterior distributions of the effect of severe damage (relative to undamaged) on annual survival (p_S) based on Model 3. The two panels illustrate the hierarchical nature of the approach where (a) is the marginal posterior distribution of the "overall" effect (i.e. $\mu_{\beta5} - \mu_{\beta3}$) describing the distribution of species' mean effects (see equation (6.14)), and (b) shows the marginal posterior distributions of each species' effect (i.e. distribution of $\beta_5 - \beta_3$ for each species).

6.4.2.3 Spatial pattern in storm intensity

The addition of the CAR model not only improves the validity of the parameter estimates by acknowledging spatial correlation in the damage data, but it also allows us to examine the spatial pattern in hurricane intensity. Negative quadrat effects (i.e. φ_1 and φ_2) indicate that there was greater damage than expected based upon the size structure (i.e. DBH of each tree) and species composition of the quadrat; positive effects reflect lower than expected damage; and, a zero effect indicates that there was no residual variation in damage after having accounted for DBH and species composition. Plots of the posterior medians for φ_1 and φ_2 (Figure 6.7) illustrate notable patchiness in storm intensities within the LFDP. The maps of the quadrat random effects indicate that the northern two thirds of the plot sustained greater levels of damage than expected compared to the southern third. This is especially the case when comparing the log odds of moderate versus severe damage (Figure 6.7(b)): the northern part has more negative effects (dark areas, higher than expected severe damage relative to moderate damage) than the southern portion (higher proportion of positive residuals, light shading).
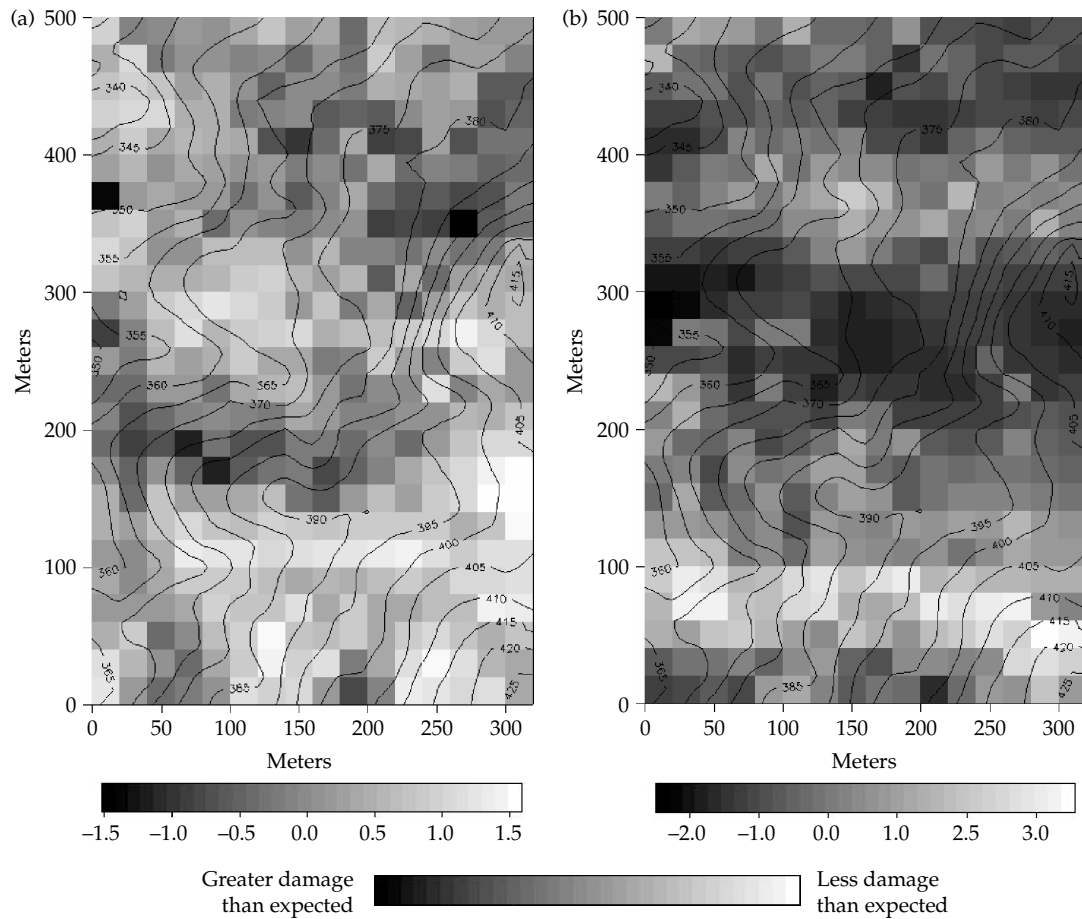
Figure 6.7. Spatial maps of the posterior medians for the damage quadrat random effects in the CAR model (φ_1 and φ_2 in equation (6.18), Model 3). The panels are (a) φ_{1k}, the residuals for the log odds of no/little versus severe damage and (b) φ_{2k}, the residuals for the log odds of moderate versus severe damage. Dark areas depict negative residuals, such that the log-odds of no damage versus severe damage (or of intermediate versus severe) is higher than expected based on the size structure (i.e. DBH) of all trees in the quadrat. White areas correspond to quadrats with lower than expected damage (positive residuals). Thus, the large black areas in the center and northern (top) part of (b) indicate regions that experienced greater damage than predicted by DBH alone, suggesting that hurricane intensity was abnormally high is these portions of the LFDP. The legend below each panel shows the gray scale associated with different numerical values for the quadrat random effects.

6.5 Discussion

6.5.1 Model comparisons

The three models that we implemented are meant to illustrate the model-building process: starting with many individual trees of a single species (Model 1), building in many individuals nested within different species (Model 2), and ending with many individuals nested within different species and spatial locations (Model 3). The parameter estimates for *C. arborea*, the only species treated in all three models, did not differ greatly between models, which is likely a result of choosing relatively noninformative hyperpriors in Model 2 and Model 3 (see equation (6.15)). If tighter densities were specified for the hyperparameters (μ_α, μ_β, the ν's), then it is likely that the parameter estimates for *C. arborea* would have differed between models. For example, if we had chosen more informative priors for $\mu_{\beta 3}$ and $\mu_{\beta 5}$ (e.g. normal densities with much smaller

variances than given in equation (6.15)) and for $\nu_{\beta 3}$ and $\nu_{\beta 5}$, then this would have resulted in (1) posterior distributions for the species-specific severe damage effects (i.e. $\beta_{5j} - \beta_{3j}$) being "pulled" toward the posterior mean that describes the distribution of species effects (i.e. $\mu_{\beta 5} - \mu_{\beta 3}$), and (2) a tighter posterior distribution for $\mu_{\beta 5} - \mu_{\beta 3}$.

Of course, Model 2 and Model 3 are preferred over Model 1 because they provide a hierarchical structure for incorporating species effects, which is of considerable importance for understanding high diversity tropical forests such as Luquillo. Model 3 is favored over Model 2 because it explicitly incorporates spatial correlation in hurricane damage, which is important because the damage probabilities exhibit nonrandom variation across the LFDP (e.g. Figure 6.7). Thus, the assumption of independence, with respect to the damage data (as in Model 2), is inappropriate and can lead to erroneous estimates of parameter uncertainty. Thus, we focus on Model 3 for the remainder of the discussion.

6.5.2 Multiple species with spatial process

The Bayesian hierarchical analysis presented here quantifies variation in species susceptibility to damage during a hurricane and susceptibility to mortality after a hurricane. The approach allows for seamless incorporation of other factors (e.g. crowding, size structure, spatial variation in damage) that are likely to influence damage experienced by and survival of each tree. Notably, the results from this analysis corroborate the idea that species-specific responses to disturbance represent an important axis in life history differentiation in tropical tree communities (Zimmerman et al. 1994).

6.5.3 Species-specific susceptibility to damage

The posteriors associated with the damage probabilities suggest that *D. excelsa* and *M. bidentata* are less likely to suffer severe damage during a hurricane compared to *A. latifolia* and *C. arborea* (Figures 6.2 and 6.3). These results are consistent with the ecological characteristics of these species. For example, species with high wood density, such as *D. excelsa* and *M. bidentata*, may be more resistant to stem damage but more likely to lose branches during a

storm (Zimmerman et al. 1994). In contrast, faster growing shade-intolerant species such as *A. latifolia* tend to have less dense wood and more slender stems and are, therefore, more susceptible to breakage (e.g. King 1986; Peltola et al. 1999). Although *C. arborea* has similar wood density to *D. excelsa*, it is more likely to tip up (Zimmerman et al. 1994), which may be partially explained by differences in rooting behavior (e.g. Harrington and DeBell 1996; Peltola et al. 1999; Stokes 1999; Cucchi et al. 2004). In the case of *D. excelsa*, extensive root grafts and anchorage to subsurface rocks provide additional stability during intense winds (Basnet et al. 1992). Additionally, of the four species considered here, *A. latifolia* and *C. arborea* are more likely to resprout after a hurricane (Zimmerman et al. 1994; Paciorek et al. 2000), and thus their ability to recover is somewhat uncoupled from the level of damage experienced during the storm.

In addition to differences among species, size classes also differ greatly with respect to susceptibility to hurricane damage. For example, across all species, smaller diameter trees are more likely to escape damage during a hurricane event (Figure 6.3(a,d,g,j)). Smaller diameter trees are also likely to be shorter and therefore to occur in the understory where neighboring large trees may provide some protection from high winds by reducing wind speeds nearer to ground level. The probability of experiencing moderate levels of damage increases with tree size (Figure 6.3(b,e,h,k)). This result agrees with previous studies, which show that beyond a certain stem diameter or tree height, size may increase the likelihood of being injured during a hurricane (Peterson and Pickett 1991; Foster and Boose 1992; Peterson and Rebertus 1997; Marks et al. 1999; Canham et al. 2001). However, the probability of suffering severe damage is nearly independent of tree size (Figure 6.3(c,f,i,l)), but this may be obscured by the fact that trees that died between Hurricane Hugo and the first census, and thus most likely suffered exceptionally severe damage, were not included in this analysis.

6.5.3.1 Species-specific posthurricane survival
As one would expect, trees that are heavily damaged during a hurricane are more likely to die following the disturbance (e.g. Figure 6.6). The sensitivity

of survival to damage appears to be a function of the life history characteristics of the species. Survival of the faster growing, shade-intolerant species *A. latifolia* and *C. arborea* is mildly affected by damage (Figure 6.5(a,b)). On the other hand, severe damage greatly reduced survival of the two shade-tolerant species *M. bidentata* (Figure 6.5(d)) and especially *D. excelsa* (Figure 6.5(c)). The pronounced effect of damage on survival of *M. bidentata* is expected because it appears to have a limited ability to resprout and its sprouts generally survive only for a short time. The few *D. excelsa* that suffer stem breakage are usually old and suffering from stem rot that causes them to break off near ground level, and thus these stems do not produce sprouts. Despite the strong negative effect of severe damage on subsequent survival of *M. bidentata* and *D. excelsa*, their overall survival is relatively high because they are fairly resistant to damage (Figure 6.3(i,l)).

Survival during the hurricane recovery period is influenced by tree size and crowding. With the exception of *D. excelsa* (for reasons noted above), survival rates were higher for larger diameter trees ($\beta_{13} < 0$; Table 6.3). This may be due to larger trees having good structural support and large labile carbon reserves that can be used for recovery from damage by producing new leaves, branches, and stem sprouts (Lieberman et al. 1985; Clark and Clark 1992; Condit et al. 1995; Blundell and Peart 2001). The effect of crowding on survival is complex and varies by species (see BA effect, β_{2j}; Table 6.3). We found negative effects of crowding on survival of *A. latifolia* ($\beta_{22} < 0$), but survival of *C. arborea* and *D. excelsa* was predicted to increase under crowded conditions (β_{21}, $\beta_{23} > 0$), and survival of *M. Bidentata* appears to be independent of basal area (i.e. the posterior distribution of β_{24} spanned a wide range of positive and negative values). These results are in contrast to previous findings that reported strong negative effects of crowding on the probability of survival following a hurricane for these four species (Zimmerman et al. 1994; Uriarte et al. 2004).

There are several potential explanations for the surprising positive correlation between survival and crowding for *C. arborea* and *D. excelsa*. First, *D. excelsa* forms extensive root grafts with conspecific neighbors (Basnet et al. 1992), which may allow for the transfer of carbohydrate resources from undamaged to damaged individuals (A. Lugo personal communication), especially in crowded stands where root grafting may be more frequent. Second, the results could also be an artifact of the timing of the censuses. The use of the initial census data with its high stem densities, including sprouts and small trees, did not take into account rapid recruitment and mortality that transpired between Hurricane Hugo and the first census. Third, the three-category classification scheme may have been insufficient to capture the range of variation in damage that each tree actually experienced. It is conceivable that dense stands reduced the effective wind speed experienced by each tree. Thus *within a given damage category*, trees in denser stands may have suffered comparably less physiological or structural injury (e.g. Harrington and DeBell 1996). This could result in reduced survival in less dense stands because the "true" level of damage suffered by trees may have been greater than similar-sized trees in denser stands.

We do not know which of the above explanations (or others not considered) are most plausible. Additional analyses that include more species, or field work after another hurricane, are needed to disentangle the factors—to determine whether there are sampling or statistical artifacts or actual biological mechanisms that contribute to the prediction that survival after a hurricane is greater in crowded stands for some species. Understanding forest dynamics will also require the use of more biologically meaningful measures of neighbor effects that extend beyond basal area as a simple index of crowding.

6.5.3.2 Spatial pattern in storm intensity

The spatial pattern in the damage quadrat random effects suggests that topographical features may amplify or dampen hurricane intensity. For example, damage by Hurricane Hugo was generally higher than expected (based on DBH and species composition) on northern exposures, ridges, and steep slopes (Figure 6.7). This is not surprising given the prevalent direction of storm tracks, the counter-clockwise spiral of hurricane winds at the land surface that generate strong winds from the northeast, and greater exposure to winds at high elevations that can cause more extensive damage on peaks and hills (Boose et al. 2004).

The spatial pattern in storm intensity also appears to reflect the land-use history at this site (see Thompson et al. 2002). For example, the northern portion of the LFDP is characterized by higher than expected levels of damage and it also experienced heavy logging and small-scale agriculture prior to 1934; active agriculture ceased after the land was purchased by the USFS in 1934. The southern third of the LFDP experienced light selective logging in the 1940s but has undergone no significant human disturbance since 1950. Hurricane disturbance may reinforce land-use legacies at this site because the species that colonize abandoned agricultural areas or gaps tend to be more vulnerable to hurricane damage than those from undisturbed habitats (Zimmerman et al. 1994; Thompson et al. 2002; Boose et al. 2004). Thus, residual variation in damage could be partially explained by the distributions of the other 40+ nonrare species not considered in this study. It is possible that the use of the quadrat random effects to estimate storm intensity may be inappropriate at this stage because these effects potentially represent convoluted interactions between land-use history, species composition, and hurricane intensity.

6.5.3.3   Future directions

Future plans involve extending Model 3 to many more species and incorporating more biologically realistic descriptions for the probabilities of suffering damage and of long-term survival. As the model becomes more complex, a hierarchical Bayesian approach becomes more and more attractive (Wikle 2003; Clark 2005) because, for example, it will allow us to obtain estimates for relatively rare species because they will "borrow strength" from common species (e.g. Gelman et al. 2004). The ability of this approach to reconstruct the spatial pattern in hurricane damage is also particularly appealing and deserves further development. For example, we assumed that φ_1 and φ_2 are independent and do not vary by species. However, φ_1 and φ_2 both describe residual variation in severe damage (relative to no/little and moderate damage), thus it is likely that they are dependent, and it is possible to model this dependency by employing a multivariate

CAR model (e.g. Banerjee et al. 2004). Moreover, risk of damage may be modified by landscape-level factors such as land-use history and topography. Thus, future work will consider landscape-level covariates within the damage model, and because some species' vulnerability to damage may be particularly sensitive to such factors, it may be appropriate to allow for species-specific CAR models.

Once landscape factors and additional species are considered in the model, this approach for quantifying spatial variation in hurricane intensity (or severity) would be preferable to methods that use the number of trees uprooted or measurements of total basal area loss because it explicitly accounts for potential effects of spatially variable species composition and size distributions. Another important contribution of this modeling approach is that it provides a means for identifying which species and size classes are most susceptible to hurricane disturbance. The approach can be easily applied to data from multiple hurricanes, varying in spatial pattern and intensity of local winds. When used with historical records of hurricane events, the resulting models can provide useful insights into the effects of varying storm regimes on forest dynamics, despite being limited in their ability to predict forest responses to winds of specific speeds.

Acknowledgments

PART IV

Spatio-temporal modeling

Spatio-temporal models are among the most challenging and relevant for environmental understanding. Chapters 7 through 9 cover a range of ways to handle the complexity of spatio-temporal interactions. In Chapter 7, Chen et al. provide background on modeling spatio-temporal variation in the context of a process—atmospheric circulation—that is, itself, spatio-temporal. In this case, two "data types," observations and model output, are simply conditioned on an underlying, unknown wind field. In other words, the wind simulation is not implemented in an inferential mode, but, rather the output is given, and inference begins there. This chapter provides background and options for non-stationary spatial processes, with technical options for modeling covariance when spatial and temporal relationships are "nonseparable."

Chapter 8 takes a different approach to spatio-temporal variation. Wikle's diffusion model of population spread is a spatio-temporal process,

with spatial variability in the diffusion coefficient itself. We have levels of spatial relationships, in the sense that movement through space varies spatially. Inference on population spread allows for the many sources of stochasticity that can affect the process and the observations thereof.

Extreme events have long been a central theme of forecasters attempting to describe and "predict" the potential for surprise. The notion of the "100-year flood" is addressed in the inferential framework with models that translate the tails of distributions into statements that may help emphasize "extremeness" in terms of frequency. In Chapter 9, Gilleland et al. take us from the classical approach for modeling extremes to the spatio-temporal context for precipitation and air quality. In a hierarchical formulation model, they allow parameters of the extreme value distribution to vary spatially. They discuss a number of considerations for modeling spatial extremes from both classical and Bayesian perspectives.